Rethinking Social Robot Navigation: Leveraging the Best of Two Worlds

Amir Hossain Raj[1*], Zichao Hu[2*], Haresh Karnan[2], Rohan Chandra[2], Amirreza Payandeh[1], Luisa Mao[2],
Peter Stone[2,3], Joydeep Biswas[2], and Xuesu Xiao[1]

Abstract— **Empowering robots to navigate in a socially compliant manner is essential for the acceptance of robots moving in human-inhabited environments. Previously, roboticists have developed geometric navigation systems with decades of empirical validation to achieve safety and efficiency. However, the many complex factors of social compliance make geometric navigation systems hard to adapt to social situations, where no amount of tuning enables them to be both safe (people are too unpredictable) and efficient (the frozen robot problem). With recent advances in deep learning approaches, the common reaction has been to entirely discard these classical navigation systems and start from scratch, building a completely new learning-based social navigation planner. In this work, we find that this reaction is unnecessarily extreme: using a large-scale real-world social navigation dataset, SCAND, we find that *geometric systems can produce trajectory plans that align with the human demonstrations in a large number of social situations*. We, therefore, ask if we can rethink the social robot navigation problem by leveraging the advantages of both geometric and learning-based methods. We validate this hybrid paradigm through a proof-of-concept experiment, in which we develop a hybrid planner that switches between geometric and learning-based planning. Our experiments on both SCAND and two physical robots show that the hybrid planner can achieve better social compliance compared to using either the geometric or learning-based approach alone.**

I. INTRODUCTION

Decades of research into autonomous mobile robot navigation allows robots to reliably move from one point to another without collision with (mostly static) obstacles [1]–[5]. Recently, there is a growing interest in bringing robots out of academic labs and into common public spaces in the wild [6]–[9]. On their way to deliver packages [6], take-outs [7], and medical supplies [8], those robots need to navigate in a way such that they not only avoid static obstacles and move towards their goals, but also take other pedestrian's objective into account. Therefore, enabling robots to navigate by social norms, known as the social robot navigation problem, has emerged as an important research topic.

To address social robot navigation, researchers have collected large-scale demonstration datasets [10]–[14], created protocols to validate social navigation systems [13]–[15], and developed social navigation techniques using geometric [16]–[24] or learning-based [25]–[33] approaches to move robots in a safe and socially compliant manner. While geometric approaches enjoy safety, explainability, and certifiabiliy, they require extensive engineering effort and
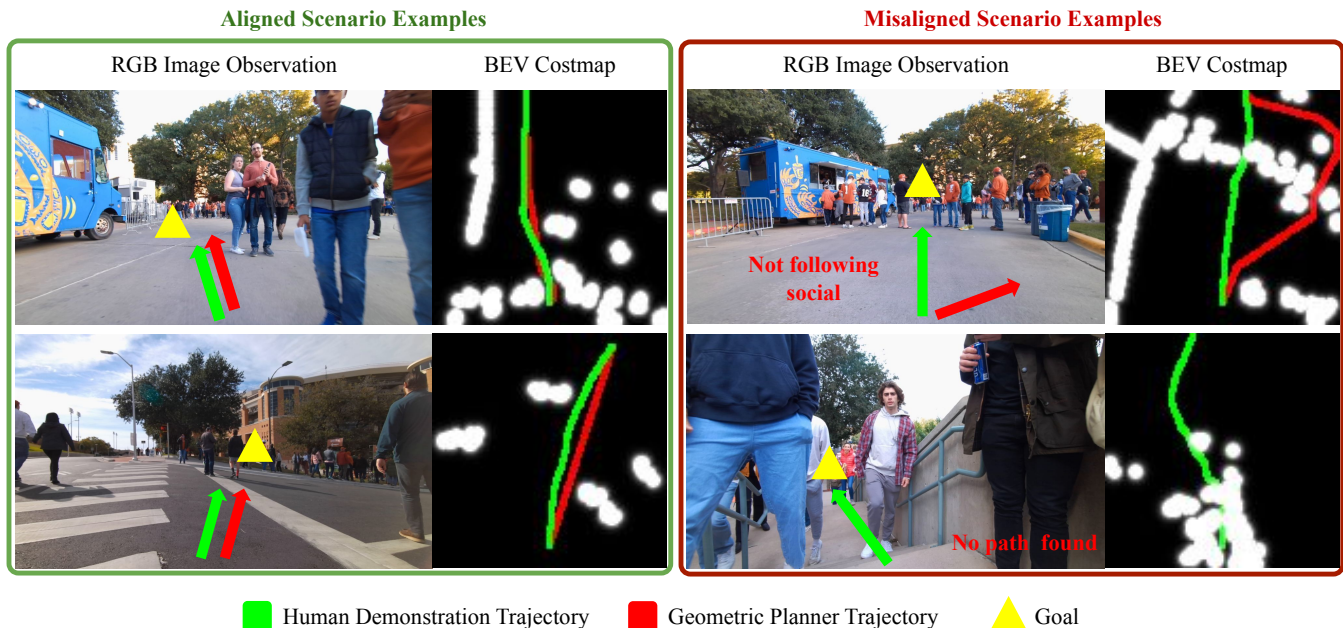

Fig. 1: Example Scenarios for Geometric Plans vs. Human Demonstrations in the SCAND dataset: In many social scenarios, the geometric planner can produce trajectories that align with human demonstration trajectories (left). While uncommon, it is inevitable for geometric planners to encounter social scenarios that they cannot handle (right). For example, the robot should approach the waiting line carefully and expect people to make room for it to pass (top right) and carefully move forward after the person on the left passes (bottom right).

*Equally contributing authors. [1] George Mason University. [2]The University of Texas at Austin. [3]Sony AI. {araj20, apayande, xiao}@gmu.edu, {zichao, haresh.miriyala, rchandra, luisa.mao}@utexas.edu, {pstone, joydeepb}@cs.texas.edu

are not scalable to complex and diverse social scenarios. On the other hand, learning-based approaches conveniently enable social navigation behaviors in a data-driven manner, but forfeit most of the benefits of their geometric counterparts. Moreover, most of these approaches have achieved improvement in social compliance primarily in experiments conducted in controlled lab environments.

Despite such academic successes, robotics practitioners are still reluctant in deploying those state-of-the-art social navigation systems on their robot fleet in the real world, especially data-driven approaches, due to their lack of safety, explainability, and testability. To the best of our knowledge, most of the navigation stacks running on real-world service robots are still geometric systems, which can be rigorously tested, confidently deployed, and easily debugged from a large-scale, real-world, software engineering perspective.

Considering the stark contrast between (i) our decade-long research and the current public resistance to mobile robots in public spaces and (ii) the active academic research in social robot navigation and the industrial reluctance to use them in real-world practices, we present a case study on social compliance of different existing robot navigation systems using a state-of-the-art Socially CompliAnt Navigation Dataset (SCAND) [10], [11] as a benchmark. We discover from the case study that geometric navigation systems can produce trajectories that align with human demonstrations in many social situations (up to 80%, e.g., Fig. 1 left). This result motivates us to rethink the approach to social robot navigation by adopting a hybrid paradigm that leverages both geometric-based and learning-based methods. We validate this paradigm by designing a proof-of-concept experiment in which we develop a hybrid planner that switches between geometric and learning-based planning. Our main contributions are:

- A social compliance definition based on how well a navigation behavior aligns with a human demonstration.
- A case study on the SCAND dataset which provides evidence that 1) geometric navigation systems can produce socially compliant navigation behaviors in many social scenarios (up to 80%, Fig. 1 left) but will inevitably fail in certain social scenarios (Fig. 1 right); and 2) learning-based methods have the potential to solve challenging social scenarios where geometric approaches fail but using them alone can suffer from distribution-shift problems.
- A hybrid paradigm that leverages both geometric-based and learning-based methods for social robot navigation. We validate this paradigm using both playback tests on SCAND and physical robot experiments on two robots.

II. BACKGROUND

A. Classical Geometric Navigation

As a research topic since decades ago, roboticists have developed a plethora of classical navigation systems to move robots from one point to another without collision with obstacles. Most classical systems take a global path from a high-level global planner, such as Dijkstra's [34], A* [35], or D* [36] algorithm, and seek help from a local planner [1], [2] to produce fine-grained motion commands

to drive robots along the global plan and avoid obstacles. Most classical navigation systems require a pre-defined cost function [37] for both global and local planning and trade off different aspects of the navigation problem, such as path length, obstacle clearance, energy consumption, and in recent years, social compliance. They then use sampling-based [1], [38], [39], optimization-based [2], [40], or potential-field-based [41] methods to generate motion commands. These approaches enjoy benefits such as safety, explainability, and testability, which can be provably or asymptotically optimal. Such benefits are important when deploying physical robots in the real world with humans around, and therefore these classical navigation systems are still widely favored by practitioners in the robot industry [6]–[9]. Implementing classical navigation approaches in socially challenging environments, however, requires substantial engineering effort such as manually designing cost functions [37] or fine-tuning navigation parameters [42]. These drawbacks motivate the use of learning-based approaches for the social robot navigation problem.

B. Learning-Based Navigation

Learning-based approaches [28], [43] may be either end-to-end [44], i.e., producing actions directly from perception, or in a structured fashion, e.g., learning local planners [45]–[52], cost functions [29], [53]–[55], kinodynamics models [56]–[58], and planner parameters [59]–[66]. From the learning perspective, most approaches fall under either imitation learning [27], [29], [44], [54], [62] from expert demonstrations or reinforcement learning [45]–[47], [52], [65], [66] from trial and error. Despite the convenience of learning emergent navigational behaviors purely from data in social scenarios, these systems suffer from the lack of safety and explainability, and cannot easily go through rigorous software testing and be debugged and fixed to avoid future failure cases. Therefore, robot practitioners rarely use learning-based navigation systems in their robot fleets deployed in the real world.

C. SCAND

SCAND [10], [11] contains 8.7 hours, 138 trajectories, and 25 miles of socially compliant, human tele-operated robot navigation demonstrations on the busy campus of The University of Texas at Austin, USA. SCAND includes socially challenging scenarios such as following, intersection, and overtaking, making it an ideal dataset to test social robot navigation methods. Additionally, SCAND provides multi-modal information, including 3D LiDAR, RGB images, joystick commands, odometry, and inertia readings, collected on two morphologically different mobile robots—a Boston Dynamics Spot and a Clearpath Jackal—controlled by four human demonstrators in indoor and outdoor environments.

III. SOCIAL COMPLIANCE CASE STUDY

In our case study, we first propose a definition of social compliance based on how well a navigation behavior aligns with the human demonstration. Then, we use this metric to benchmark the social compliance of a set of geometric

navigation systems on SCAND. Three major findings from these analyses are:

1) Different geometric navigation systems show similar performance, where their trajectories align with human demonstrations in up to 80% SCAND scenarios.
2) A general purpose navigation planner, e.g., move_base, even without tuning for specific scenarios can often produce trajectories aligning with human demonstrations.
3) Despite the inevitable failures of geometric navigation planners that cannot be resolved through manual tuning, such occurrences remain infrequent within SCAND.

Finally, we investigate the performance of geometric-based and learning-based planners on both an in-distribution and out-of-distribution test set and find that training on SCAND can suffer from distribution-shift problems.

A. Defining Social Compliance on SCAND

SCAND is a dataset designed for learning from demonstration research, so we assume the human demonstrations provided in the dataset to be the ground truth[1]. In this work, we propose a definition of social compliance based on how well a navigation behavior produced by a navigation system aligns with the human demonstration.

Definition 1: Given a navigation scenario $\mathcal{S}_t$ with a human demonstration behavior $\mathcal{B}_t^D$ at a time step t, a navigation behavior $\mathcal{B}_t$ is **socially compliant** if $d = \|\mathcal{B}_t - \mathcal{B}_t^D\|_D < \epsilon$, where $\|\cdot\|_D$ is a distance metric and ϵ is a small threshold.

In this work, we define the navigation scenario $\mathcal{S}_t$ to be the robot sensor observations in the past two seconds at a certain time step t of a demonstration trajectory in SCAND. We also define human demonstration behavior $\mathcal{B}_t^D$ as a deterministic sequence of waypoints, $P_i^D = (x_i^D, y_i^D)$, at every step i starting from time step t, to a navigation goal, $P_{t_g}^D$, 10m ahead of the robot at time step t_g on the human demonstrated path: $\mathcal{B}_t^D = \{P_i^D\}_{i=t}^{t_g}$, where t_g is the first time step when $\|P_t^D - P_{t_g}^D\| \geq 10$. Then we send the same navigation goal, $P_{t_g}^D$, to a navigation system to be benchmarked and retrieve its planned trajectory $\mathcal{B}_t$. Finally, considering most geometric navigation systems use a global trajectory planner before local motion planning and the quality of the robot motions heavily depends on the quality of the planned global trajectories $\mathcal{B}_t$, we use the undirected Hausdorff distance, which measures the distance from each point in the planned trajectory $\mathcal{B}_t$ to the closest point in the corresponding demonstration trajectory $\mathcal{B}_t^D$ as $\|\cdot\|_D$, to measure the social compliance of the planned trajectory:

$$d = \max\{ \sup_{P_i^D \in \mathcal{B}_t^D} \inf_{P_i \in \mathcal{B}_t} \|P_i^D - P_i\|, \\ \sup_{P_i \in \mathcal{B}_t} \inf_{P_i^D \in \mathcal{B}_t^D} \|P_i^D - P_i\|\}.$$

Fig. 2 shows trajectories with different Hausdorff distances from a Bird's Eye View (BEV). Empirically, navigation systems that align better with human demonstrations are expected to yield a lower Hausdorff distance.

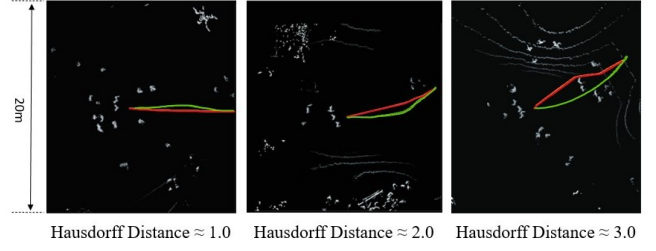Hausdorff Distance ≈ 1.0   Hausdorff Distance ≈ 2.0   Hausdorff Distance ≈ 3.0

Fig. 2: Different Hausdorff distances between the human demonstration trajectory (green) and geometric planner trajectory (red). White dots denote nearby humans and obstacles. Empirically, navigation systems that align better with human demonstrations are expected to yield a lower Hausdorff distance.
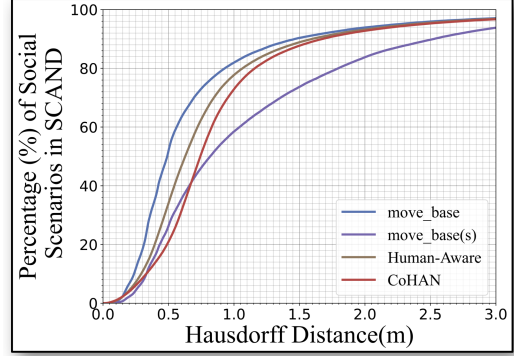

Fig. 3: Cumulative Distribution Function (CDF) curves illustrating the Hausdorff distance and social scenario percentages for four distinct geometric planners, analyzed on the SCAND.

B. Geometric Navigation Systems

We benchmark the social compliance of four publicly available geometric navigation systems on SCAND:

1) move_base [67]: The Robot Operating System (ROS) move_base is a well-known geometric navigation system that consists of a global planner and a local planner. The global planner uses Dijkstra's algorithm to plan an optimal trajectory on a static costmap and the local planner then employs the Dynamic Window Approach (DWA) [1] to generate real-time actions given the global trajectory.

2) move_base with social layer (move_base(s)) [68]: This method enhances move_base by incorporating a social layer into the static costmap. It leverages real-time LiDAR scans to identify humans and surrounds them with a Gaussian filter for improved social awareness in planning.

3) Human-Aware Planner [20]: The Human-Aware Planner introduces a social cost function into path planning to prioritize human comfort and ensure politeness and safety. It uses time-dependent and kinodynamic path planning to consider the spatial relationship of the robot and humans.

4) CoHAN [19]: CoHAN is a human-aware navigation planner that uses an extension of the Human-Aware Timed Elastic Band (HATEB) planner [69] as the local planner to handle complex and crowded navigation scenarios. This system is developed over the ROS navigation stack by introducing human safety and human visibility costmap layers into both global and local costmap.

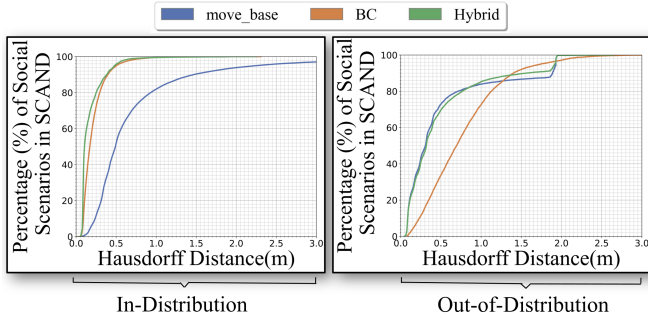We maintain the default parameterizations and configura-

Fig. 4: CDF curves of Geometric, Learning-Based, and Proposed Hybrid Navigation Planners on In-Distribution SCAND and Out-of-Distribution Test Data.

tions for all four geometric navigation systems. Each system is evaluated by playing back SCAND data, recording the planned trajectories $\mathcal{B}_t$, and comparing them against the SCAND demonstration trajectories $\mathcal{B}_t^D$ to evaluate their social compliance under Def. 1.

Fig. 3 illustrates four Cumulative Distribution Function (CDF) curves comparing the performance of the four geometric navigation systems, indicating consistent trends among the systems: across many social scenarios in SCAND, they manage to maintain a moderate deviation from human demonstrations within $\epsilon = 1.0$. We find that move_base achieves the best alignment with human demonstrations in over 80% of SCAND navigation scenarios. This outcome is unexpected, given that move_base is the only navigation system among those evaluated that does not explicitly incorporate social factors into its algorithm. This observation suggests that a general-purpose navigation planner even without tuning for specific social scenarios can often produce socially compliant trajectories.

Additionally, we observe a small portion (roughly 5%) of scenarios where the geometric planners deviate significantly from human demonstrations (more than 3 meters Hausdorff distance). To understand the causes of such deviations, we sample 50 of these scenarios and inspect the interactions between the robot and the environment. We discover that these scenarios often require sophisticated reasoning skills that a geometric planner does not possess. For example, Fig. 1 shows two common social scenarios that are challenging for geometric planners and inevitably lead to poor compliance.

C. Comparing Geometric and Learning-Based Planner

In social robot navigation, human behaviors are unpredictable and the environment can vary significantly at different locations and times. Hence, it is challenging to create one dataset to capture the full distributions of social scenarios. This limitation could cause learning-based methods to suffer from the distribution-shift problem [70].

In order to investigate this problem, in addition to training and testing on SCAND, we follow SCAND's procedure and collect extra demonstrations as an out-of-distribution test set. These demonstrations contain manually curated social scenarios in a lab environment, including intersection encounter, frontal approach, and people following. We then train a simple learning-based method, Behavior Cloning (BC) [71],

on the SCAND training set and evaluate its performance on both the in-distribution SCAND test set and the manually curated out-of-distribution test set. Finally, we compare it with a general-purpose geometric planner, move_base, on both in-distribution and out-of-distribution data.

We plot the CDFs of the percentage of social scenarios over different Hausdorff distance thresholds in Fig. 4. We observe that while BC can outperform move_base on the in-distribution SCAND test data, BC's performance significantly deteriorates on the out-of-distribution test set. move_base's performance remains unchanged. This result indicates that training on the SCAND dataset might be affected by the distribution-shift problem, leading to poor generalization when facing various unseen social scenarios.

IV. RETHINKING SOCIAL ROBOT NAVIGATION

Our case study results suggest 1) geometric navigation systems can produce socially compliant navigation behaviors in many social scenarios but will inevitably fail in certain social scenarios; and 2) learning-based methods (in our case, BC) have the potential to solve challenging social scenarios where geometric approaches fail but using them alone can suffer from distribution-shift problems.

Our case study motivates us to rethink the approach to solving social robot navigation: can we take advantage of both geometric and learning-based approaches? In this work, we make an initial exploratory effort to answer this question: we develop a hybrid planner that uses a geometric navigation system as the backbone and complements it with a learned model (BC) for handling difficult social navigation scenarios. We also train a classifier to serve as a gating function, determining when move_base is likely to fail at generating a socially compliant behavior, at which point we switch to using the output from BC. To be specific, let S_t be a social scenario at time step t. We instantiate our hybrid navigation planner $\mathcal{F}(\cdot)$ based on a geometric navigation planner $\mathcal{C}(\cdot)$, a learning-based planner $\mathcal{L}_\theta(\cdot)$ with learnable parameters θ, and a gating function $\mathcal{G}_\phi(\cdot)$ with learnable parameters ϕ that selects between the output from the geometric and learning-based planners:

$$\mathcal{B}_t = \mathcal{F}(\mathcal{S}_t) = \mathcal{G}_\phi(\mathcal{C}(\mathcal{S}_t), \mathcal{L}_\theta(\mathcal{S}_t), \mathcal{S}_t).$$

The parameters ϕ and θ can be learned using supervised learning on the navigation scenario and behavior tuples $\{\mathcal{S}_t, \mathcal{B}_t^D\}_{t=1}^T$ in SCAND:

$$\underset{\phi, \theta}{\arg\min} \sum_{t=1}^T d(\mathcal{S}_t),$$
$$d(\mathcal{S}_t) = \|\mathcal{B}_t - \mathcal{B}_t^D\|,$$
$$\mathcal{B}_t = \mathcal{G}_\phi(\mathcal{C}(\mathcal{S}_t), \mathcal{L}_\theta(\mathcal{S}_t), \mathcal{S}_t).$$

Among the many ways to learn $\mathcal{G}_\phi(\cdot)$ and $\mathcal{L}_\theta(\cdot)$ (either jointly or separately), in this work, we present a simple implementation that first learns a classifier $\mathcal{M}_\phi(\mathcal{S}_t)$ based on the difference d between $\mathcal{B}_t^D$ and $\mathcal{C}(\mathcal{S}_t)$ to choose between $\mathcal{C}(\mathcal{S}_t)$ and $\mathcal{L}_\theta(\mathcal{S}_t)$:

$$\mathcal{B}_t = \begin{cases} \mathcal{C}(\mathcal{S}_t), & \text{if } \mathcal{M}_\phi(\mathcal{S}_t) = 1, \\ \mathcal{L}_\theta(\mathcal{S}_t), & \text{if } \mathcal{M}_\phi(\mathcal{S}_t) = 0. \end{cases}$$
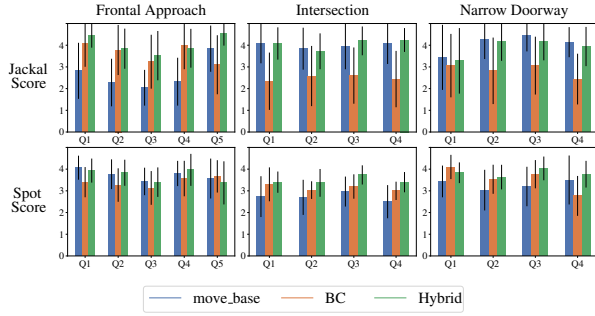
Fig. 5: Human Study Average Scores Per Question.

Jackal	Frontal	Intersection	Doorway
move_base	2.66 ± 0.64	3.98 ± 0.10	$\mathbf{4.08 \pm 0.38}$
BC	3.63 ± 0.40	2.49 ± 0.11	2.84 ± 0.25
Hybrid	$\mathbf{4.04 \pm 0.39}$	$\mathbf{4.06 \pm 0.20}$	3.89 ± 0.36
Spot	**Frontal**	**Intersection**	**Doorway**
move_base	$\mathbf{3.73 \pm 0.22}$	2.72 ± 0.17	3.29 ± 0.19
BC	3.41 ± 0.19	3.13 ± 0.12	3.54 ± 0.49
Hybrid	3.70 ± 0.26	$\mathbf{3.48 \pm 0.15}$	$\mathbf{3.82 \pm 0.14}$

TABLE I: Human Study Average Scores Per Method and Scenario: Participants generally prefer the robot with the hybrid approach to the pure classical or the pure BC approach.

$\mathcal{C}(\cdot)$ can already produce socially compliant behaviors when $d \leq \epsilon$, while $\mathcal{L}_\theta(\cdot)$ only learns to address navigation scenarios where $d > \epsilon$. By comparing $\mathcal{C}(\mathcal{S}_t)$ against $\mathcal{B}_t^D$, i.e., $d = ||\mathcal{C}(\mathcal{S}_t) - \mathcal{B}_t^D||$, we separate the original SCAND $\mathcal{D}$ into a socially compliant, $\mathcal{D}^C$, and a socially non-compliant, $\mathcal{D}^N$, subset with respect to $\mathcal{C}(\cdot)$, and form a supervised dataset $\{\mathcal{S}_t, c_t\}_{t=1}^T$, in which $c_t = 1$ if $\mathcal{S}_t \in \mathcal{D}^C$ ($d \leq \epsilon$) and $c_t = 0$ if $\mathcal{S}_t \in \mathcal{D}^N$ ($d > \epsilon$). Then, $\mathcal{M}_\phi(\cdot)$ is learned via supervised learning with a cross-entropy loss to classify whether $\mathcal{C}(\mathcal{S}_t)$ is socially compliant or not:

$$\phi^* = \operatorname*{argmax}_{\phi} \sum_{t=1}^T \log \frac{\exp(\mathcal{M}_\phi(\mathcal{S}_t)[c_t])}{\exp(\mathcal{M}_\phi(\mathcal{S}_t)[0]) + \exp(\mathcal{M}_\phi(\mathcal{S}_t)[1])}.$$

The learning-based planner $\mathcal{L}_\theta$ is then learned to minimize the difference between its outputs and demonstrations in $\mathcal{D}^N$:

$$\theta^* = \operatorname*{argmin}_{\theta} \sum_{(\mathcal{S}_t, \mathcal{B}_t^D) \in \mathcal{D}^N} ||\mathcal{L}_\theta(\mathcal{S}_t) - \mathcal{B}_t^D||.$$

During deployment, $\mathcal{F}(\cdot)$ first uses $\mathcal{M}_{\phi^*}(\cdot)$ to classify if $\mathcal{C}(\mathcal{S}_t)$ is socially compliant or not, and then executes $\mathcal{C}(\mathcal{S}_t)$ if compliant or $\mathcal{L}_{\theta^*}(\mathcal{S}_t)$ if not.

We evaluate the hybrid planner on both the in-distribution and out-of-distribution test sets and compare it with the geometric and BC planners. Fig. 4 shows the hybrid planner performs similarly to the best-performing planner on either test set, suggesting that the hybrid planner can take advantage of the best of both worlds during the playback tests.

V. PHYSICAL EXPERIMENTS

We conduct a human study in a series of physical experiments to assess the social compliance of our proposed hybrid approach, in comparison to an existing classical planner,

i.e., move_base, and an end-to-end learning-based method, i.e., BC trained on SCAND. The experiments are conducted using a wheeled Clearpath Jackal and a legged Boston Dynamics Spot to show the generalizability of our proposed hybrid approach to robots with different morphologies on two university campuses, George Mason University (GMU) and The University of Texas at Austin (UT), respectively. We test the robots' social compliance within three distinct social scenarios, i.e., Frontal Approach, Intersection, and Narrow Doorway. We keep the same setup of our hybrid approach among all three scenarios. The three methods are randomly shuffled and repeated five times, and human participants are requested to respond to a questionnaire with 4-5 questions using Likert scales [15], [29] following each run. Each scenario is tested on ten different individuals (fifteen interactions per individual).

A. Social Compliance Questionnaire

For Frontal Approach, the five questions are[2]:

1) *The robot moved to avoid me.*
2) *The robot obstructed my path**.
3) *The robot maintained a safe and comfortable distance at all times.*
4) *The robot nearly collided with me**.
5) *It was clear what the robot wanted to do.*

For Intersection, the four questions are:

1) *The robot let me cross the intersection by maintaining a safe and comfortable distance.*
2) *The robot changed course to let me pass.*
3) *The robot paid attention to what I was doing.*
4) *The robot slowed down and stopped to let me pass.*

For Narrow Doorway, the four questions are:

1) *The robot got in my way**.
2) *The robot moved to avoid me.*
3) *The robot made room for me to enter or exit.*
4) *It was clear what the robot wanted to do.*

The quantitative results of our experiments are shown in Fig. 5, where we plot the per-question average along with error bars for the three methods in each of the scenarios.

B. Engineering Endeavors During Deployment

When deploying the hybrid planner on the robots, we incorporate a voting system that employs hysteresis by considering the past n time steps with a threshold value of r to switch between planners. To prevent collisions, we set a strict condition: if the robots get within p meters of an obstacle, they immediately switch to the geometric planner for the next t seconds. We empirically set the values for n, r, p, and t depending on the location and robot. These adjustments make our hybrid system more stable and safer when running on real robots.

---

[2]* denotes negatively formulated questions, for which we reverse-code the ratings to make them comparable to the positively formulated ones.

Fig. 6: GMU Jackal Frontal Approach (Left) and UT Spot Narrow Doorway (Right) Robot Experiments.

C. Jackal Experiments at GMU

For the experiments at GMU with the wheeled Jackal, our hybrid method shows the most distinguishable social behavior for the frontal approach, maintaining a safe distance while passing by another person coming straight from the opposite side. For the other two scenarios, the classifier of our hybrid method mostly commands to stick to the classical planner and therefore we see similar performance of the classical and our hybrid approach. On the other hand, BC is inconsistent in the majority of the runs: Either it cannot reach the goal successfully, which is evident in the low BC scores for Jackal Frontal Approach Q5 (Fig. 5 top left) and Jackal Narrow Doorway Q4 (Fig. 5 top right), or we have to manually intervene to avoid an imminent collision with the human subject or surroundings. Across the different scenarios, we observe that our approach remains consistent by maintaining the highest average in most of the questions. With both GMU and UT experiments, we ran a one-way ANOVA test on the data from each question with three groups, and the test confirms the statistical significance of the comparison at a 95% confidence level. We show the Jackal Frontal Approach experiment in Fig. 6 left as an example: Classical approach follows a trajectory which passes very close to the human; BC avoids the human but it cannot recover back to the correct trajectory and gets too close to the wall before we manually intervene; Hybrid approach reacts early by maintaining a safe distance to the human (using BC) and successfully reaches the goal (using move_base).

D. Spot Experiments at UT Austin

We also conduct experiments with a legged Spot at UT. In general, we observe our hybrid approach still performs the most consistently across all three scenarios. However, the classical planner's performance is slightly worse compared to the GMU Jackal experiments. It does not perform well on Spot Intersection (Fig. 5 lower middle) and Spot Narrow Doorway (Fig. 5 lower right, except Q4 since unlike BC, the classical approach can always reach the goal). We posit this is caused by the different motion morphology of the Spot: legged robots are holonomic, and like humans it is possible for them to side-step during a social interaction. Not

being able to do so due to the limitation of move_base may cause its movement to be perceived unnatural. BC performs slightly better for Spot in Intersection (Fig. 5 lower middle) and Narrow Doorway (Fig. 5 lower right). We show the Spot Narrow Doorway experiment in Fig. 6 right as an example: Classical approach first follows the shortest path until it gets close to the human and avoids the human; BC avoids the human but gets lost thereafter; Hybrid approach can slow down and avoid the human in the beginning and successfully pass the narrow doorway in the end.

VI. Conclusions, Limitations, and Future Work

This work presents a case study on benchmarking social compliance of different existing geometric navigation systems using the SCAND dataset. Our case study results suggest 1) geometric navigation systems can produce socially compliant navigation behaviors in many social scenarios (up to 80%) but will inevitably fail in certain social scenarios; and 2) learning-based methods (in our case, BC) have the potential to solve challenging social scenarios where geometric approaches fail but using them alone can suffer from distribution-shift problems. These findings motivate us to rethink social robot navigation: we propose a hybrid paradigm that leverages both geometric-based and learning-based planners. We develop a hybrid planner and evaluate its performance both in the playback tests and on two physical robots as a proof-of-concept experiment. The experiment shows promising results of the hybrid paradigm.

This work has several limitations. First, getting the system working robustly during deployment poses engineering challenges. It requires further investigation to understand how to integrate geometric-based and learning-based methods better. In addition, the BC algorithm used in this work is a straightforward representative of a variety of learning-based methods, which can be replaced by more sophisticated model designs. Overall, this work serves as a preliminary effort to rethink social robot navigation with a hybrid paradigm and to inspire further investigation of this paradigm in the future.

VII. Acknowledgements

References

[1] D. Fox, W. Burgard, and S. Thrun, "The dynamic window approach to collision avoidance," *IEEE Robotics & Automation Magazine*, vol. 4, no. 1, pp. 23–33, 1997.

[2] S. Quinlan and O. Khatib, "Elastic bands: Connecting path planning and control," in *[1993] Proceedings IEEE International Conference on Robotics and Automation*. IEEE, 1993, pp. 802–807.

[3] X. Xiao, Z. Xu, Z. Wang, Y. Song, G. Warnell, P. Stone, T. Zhang, S. Ravi, G. Wang, H. Karnan *et al.*, "Autonomous ground navigation in highly constrained spaces: Lessons learned from the benchmark autonomous robot navigation challenge at icra 2022 [competitions]," *IEEE Robotics & Automation Magazine*, vol. 29, no. 4, pp. 148–156, 2022.

[4] D. Perille, A. Truong, X. Xiao, and P. Stone, "Benchmarking metric ground navigation," in *2020 IEEE International Symposium on Safety, Security, and Rescue Robotics (SSRR)*. IEEE, 2020, pp. 116–121.

[5] A. Nair, F. Jiang, K. Hou, Z. Xu, S. Li, X. Xiao, and P. Stone, "Dynabarn: Benchmarking metric ground navigation in dynamic environments," in *2022 IEEE International Symposium on Safety, Security, and Rescue Robotics (SSRR)*. IEEE, 2022, pp. 347–352.

[6] Amazon, "Meet scout," www.aboutamazon.com/news/transportation/meet-scout, 2022.

[7] Starship, "Starship," www.starship.xyz/, 2022.

[8] Dilligent Robotics, "Dilligent robotics," www.diligentrobots.com/, 2022.

[9] Tiny Mile, "Tiny mile," tinymile.ai/, 2022.

[10] H. Karnan, A. Nair, X. Xiao, G. Warnell, S. Pirk, A. Toshev, J. Hart, J. Biswas, and P. Stone, "Socially Compliant Navigation Dataset (SCAND): A Large-Scale Dataset of Demonstrations for Social Navigation," *IEEE Robotics and Automation Letters*, 2022.

[11] ——, "Socially Compliant Navigation Dataset (SCAND)," *Texas Data Repository*, 2022. [Online]. Available: https://doi.org/10.18738/T8/0PRYRH

[12] D. M. Nguyen, M. Nazeri, A. Payandeh, A. Datar, and X. Xiao, "Toward human-like social robot navigation: A large-scale, multi-modal, social human navigation dataset," in *2023 IEEE/RSJ International Conference on Intelligent Robots and Systems (IROS)*. IEEE, 2023.

[13] A. Francis, C. Pérez-D'Arpino, C. Li, F. Xia, A. Alahi, A. Bera, A. Biswas, J. Biswas, H.-T. L. Chiang, M. Everett, S. Ha, J. Hart, H. Karnan, T.-W. E. Lee, L. J. Manso, R. Mirsky, S. Pirk, P. T. Singamaneni, P. Stone, A. Taylor, P. Trautman, N. Tsoi, M. Vázquez, X. Xiao, P. Xu, N. Yokoyama, R. Martín-Martín, and A. Toshev, "Benchmarking social robot navigation across academia and industry," in *Proceedings of the AAAI 2023 Spring Symposium on HRI in Academia and Industry: Bridging the Gap*. AAAI, 2023.

[14] A. Francis, C. Pérez-d'Arpino, C. Li, F. Xia, A. Alahi, R. Alami, A. Bera, A. Biswas, J. Biswas, R. Chandra *et al.*, "Principles and guidelines for evaluating social robot navigation algorithms," *arXiv preprint arXiv:2306.16740*, 2023.

[15] S. Pirk, E. Lee, X. Xiao, L. Takayama, A. Francis, and A. Toshev, "A protocol for validating social navigation policies," in *2022 IEEE international conference on robotics and automation (ICRA) Workshop on Social Robot Navigation: Advances and Evaluation*. IEEE, 2022.

[16] R. Kirby, *Social robot navigation*. Carnegie Mellon University, 2010.

[17] R. Mirsky, X. Xiao, J. Hart, and P. Stone, "Conflict avoidance in social navigation–a survey," *arXiv preprint arXiv:2106.12113*, 2021.

[18] J. Hart, R. Mirsky, X. Xiao, S. Tejeda, B. Mahajan, J. Goo, K. Baldauf, S. Owen, and P. Stone, "Using human-inspired signals to disambiguate navigational intentions," in *International Conference on Social Robotics*. Springer, 2020, pp. 320–331.

[19] P. T. Singamaneni, A. Favier, and R. Alami, "Human-aware navigation planner for diverse human-robot ineraction contexts," in *IEEE/RSJ International Conference on Intelligent Robots and Systems (IROS)*, 2021.

[20] M. Kollmitz, K. Hsiao, J. Gaa, and W. Burgard, "Time dependent planning on a layered social cost map for human-aware robot navigation," in *2015 European Conference on Mobile Robots (ECMR)*. IEEE, 2015, pp. 1–6.

[21] R. Chandra, V. Zinage, E. Bakolas, J. Biswas, and P. Stone, "Decentralized multi-robot social navigation in constrained environments via game-theoretic control barrier functions," *arXiv preprint arXiv:2308.10966*, 2023.

[22] R. Chandra, R. Maligi, A. Anantula, and J. Biswas, "Socialmapf: Optimal and efficient multi-agent path finding with strategic agents for social navigation," *IEEE Robotics and Automation Letters*, 2023.

[23] R. Chandra, R. Menon, Z. Sprague, A. Anantula, and J. Biswas, "Decentralized social navigation with non-cooperative robots via bi-level optimization," *arXiv preprint arXiv:2306.08815*, 2023.

[24] J. Holtz, S. Andrews, A. Guha, and J. Biswas, "Iterative program synthesis for adaptable social navigation," in *2021 IEEE/RSJ International Conference on Intelligent Robots and Systems (IROS)*. IEEE, 2021, pp. 6256–6261.

[25] C. Rösmann, M. Oeljeklaus, F. Hoffmann, and T. Bertram, "Online trajectory prediction and planning for social robot navigation," in *2017 IEEE International Conference on Advanced Intelligent Mechatronics (AIM)*. IEEE, 2017, pp. 1255–1260.

[26] Y. F. Chen, M. Everett, M. Liu, and J. P. How, "Socially aware motion planning with deep reinforcement learning," in *2017 IEEE/RSJ International Conference on Intelligent Robots and Systems (IROS)*. IEEE, 2017, pp. 1343–1350.

[27] H. Karnan, G. Warnell, X. Xiao, and P. Stone, "Voila: Visual-observation-only imitation learning for autonomous navigation," in *2022 International Conference on Robotics and Automation (ICRA)*. IEEE, 2022, pp. 2497–2503.

[28] X. Xiao, B. Liu, G. Warnell, and P. Stone, "Motion planning and control for mobile robot navigation using machine learning: a survey," *Autonomous Robots*, vol. 46, no. 5, pp. 569–597, 2022.

[29] X. Xiao, T. Zhang, K. M. Choromanski, T.-W. E. Lee, A. Francis, J. Varley, S. Tu, S. Singh, P. Xu, F. Xia, S. M. Persson, L. Takayama, R. Frostig, J. Tan, C. Parada, and V. Sindhwani, "Learning model predictive controllers with real-time attention for real-world navigation," in *Conference on robot learning*. PMLR, 2022.

[30] J.-S. Park, X. Xiao, G. Warnell, H. Yedidson, and P. Stone, "Learning perceptual hallucination for multi-robot navigation in narrow hallways," in *2023 IEEE International Conference on Robotics and Automation (ICRA)*. IEEE, 2023, pp. 10 033–10 039.

[31] J. Holtz, S. Andrews, A. Guha, and J. Biswas, "Iterative program synthesis for adaptable social navigation," in *Intelligent Robots and Systems (IROS), IEEE/RSJ International Conference on*, 2021, pp. 6256–6261.

[32] J. Holtz and J. Biswas, "Socialgym: A framework for benchmarking social robot navigation," 2022.

[33] Z. Sprague, R. Chandra, J. Holtz, and J. Biswas, "Socialgym 2.0: Simulator for multi-agent social robot navigation in shared human spaces," *arXiv preprint arXiv:2303.05584*, 2023.

[34] E. W. Dijkstra, "A note on two problems in connexion with graphs," *Numerische mathematik*, vol. 1, no. 1, pp. 269–271, 1959.

[35] P. E. Hart, N. J. Nilsson, and B. Raphael, "A formal basis for the heuristic determination of minimum cost paths," *IEEE transactions on Systems Science and Cybernetics*, vol. 4, no. 2, pp. 100–107, 1968.

[36] D. Ferguson and A. Stentz, "Using interpolation to improve path planning: The field d* algorithm," *Journal of Field Robotics*, vol. 23, no. 2, pp. 79–101, 2006.

[37] D. V. Lu, D. Hershberger, and W. D. Smart, "Layered costmaps for context-sensitive navigation," in *2014 IEEE/RSJ International Conference on Intelligent Robots and Systems*. IEEE, 2014, pp. 709–715.

[38] L. E. Kavraki, P. Svestka, J.-C. Latombe, and M. H. Overmars, "Probabilistic roadmaps for path planning in high-dimensional configuration spaces," *IEEE Transactions on Robotics and Automation*, vol. 12, no. 4, pp. 566–580, 1996.

[39] J. J. Kuffner and S. M. LaValle, "Rrt-connect: An efficient approach to single-query path planning," in *Proceedings 2000 ICRA. Millennium Conference. IEEE International Conference on Robotics and Automation. Symposia Proceedings (Cat. No. 00CH37065)*, vol. 2. IEEE, 2000, pp. 995–1001.

[40] N. Ratliff, M. Zucker, J. A. Bagnell, and S. Srinivasa, "Chomp: Gradient optimization techniques for efficient motion planning," in *2009 IEEE international conference on robotics and automation*. IEEE, 2009, pp. 489–494.

[41] Y. Koren, J. Borenstein *et al.*, "Potential field methods and their inherent limitations for mobile robot navigation." in *Icra*, vol. 2, no. 1991, 1991, pp. 1398–1404.

[42] K. Zheng, "Ros navigation tuning guide," *Robot Operating System (ROS) The Complete Reference (Volume 6)*, pp. 197–226, 2021.

[43] A. Payandeh, K. T. Baghaei, P. Fayyazsanavi, S. B. Ramezani, Z. Chen, and S. Rahimi, "Deep representation learning: Fundamentals, technologies, applications, and open challenges," *IEEE Access*, vol. 11, pp. 137 621–137 659, 2023.

[44] Y. Pan, C.-A. Cheng, K. Saigol, K. Lee, X. Yan, E. A. Theodorou, and B. Boots, "Imitation learning for agile autonomous driving," *The*

International Journal of Robotics Research, vol. 39, no. 2-3, pp. 286–302, 2020.

[45] A. Faust, K. Oslund, O. Ramirez, A. Francis, L. Tapia, M. Fiser, and J. Davidson, "Prm-rl: Long-range robotic navigation tasks by combining reinforcement learning and sampling-based planning," in *2018 IEEE International Conference on Robotics and Automation (ICRA)*. IEEE, 2018, pp. 5113–5120.

[46] H.-T. L. Chiang, A. Faust, M. Fiser, and A. Francis, "Learning navigation behaviors end-to-end with autorl," *IEEE Robotics and Automation Letters*, vol. 4, no. 2, pp. 2007–2014, 2019.

[47] A. Francis, A. Faust, H.-T. L. Chiang, J. Hsu, J. C. Kew, M. Fiser, and T.-W. E. Lee, "Long-range indoor navigation with prm-rl," *IEEE Transactions on Robotics*, vol. 36, no. 4, pp. 1115–1134, 2020.

[48] X. Xiao, B. Liu, G. Warnell, and P. Stone, "Toward agile maneuvers in highly constrained spaces: Learning from hallucination," *IEEE Robotics and Automation Letters*, vol. 6, no. 2, pp. 1503–1510, 2021.

[49] X. Xiao, B. Liu, and P. Stone, "Agile robot navigation through hallucinated learning and sober deployment," in *2021 IEEE international conference on robotics and automation (ICRA)*. IEEE, 2021, pp. 7316–7322.

[50] Z. Wang, X. Xiao, A. J. Nettekoven, K. Umasankar, A. Singh, S. Bommakanti, U. Topcu, and P. Stone, "From agile ground to aerial navigation: Learning from learned hallucination," in *2021 IEEE/RSJ International Conference on Intelligent Robots and Systems (IROS)*. IEEE, 2021, pp. 148–153.

[51] B. Liu, X. Xiao, and P. Stone, "A lifelong learning approach to mobile robot navigation," *IEEE Robotics and Automation Letters*, vol. 6, no. 2, pp. 1090–1096, 2021.

[52] Z. Xu, B. Liu, X. Xiao, A. Nair, and P. Stone, "Benchmarking reinforcement learning techniques for autonomous navigation," in *2023 IEEE International Conference on Robotics and Automation (ICRA)*. IEEE, 2023.

[53] N. Pérez-Higueras, R. Ramón-Vigo, F. Caballero, and L. Merino, "Robot local navigation with learned social cost functions," in *2014 11th International Conference on Informatics in Control, Automation and Robotics (ICINCO)*, vol. 2. IEEE, 2014, pp. 618–625.

[54] M. Wigness, J. G. Rogers, and L. E. Navarro-Serment, "Robot navigation from human demonstration: Learning control behaviors," in *2018 IEEE International Conference on Robotics and Automation (ICRA)*. IEEE, 2018, pp. 1150–1157.

[55] K. S. Sikand, S. Rabiee, A. Uccello, X. Xiao, G. Warnell, and J. Biswas, "Visual representation learning for preference-aware path planning," in *2022 International Conference on Robotics and Automation (ICRA)*. IEEE, 2022, pp. 11 303–11 309.

[56] X. Xiao, J. Biswas, and P. Stone, "Learning inverse kinodynamics for accurate high-speed off-road navigation on unstructured terrain," *IEEE Robotics and Automation Letters*, vol. 6, no. 3, pp. 6054–6060, 2021.

[57] H. Karnan, K. S. Sikand, P. Atreya, S. Rabiee, X. Xiao, G. Warnell, P. Stone, and J. Biswas, "Vi-ikd: High-speed accurate off-road navigation using learned visual-inertial inverse kinodynamics," in *2022 IEEE/RSJ International Conference on Intelligent Robots and Systems (IROS)*. IEEE, 2022, pp. 3294–3301.

[58] P. Atreya, H. Karnan, K. S. Sikand, X. Xiao, S. Rabiee, and J. Biswas, "High-speed accurate robot control using learned forward kinodynamics and non-linear least squares optimization," in *2022 IEEE/RSJ International Conference on Intelligent Robots and Systems (IROS)*. IEEE, 2022, pp. 11 789–11 795.

[59] D. Teso-Fz-Betoño, E. Zulueta, U. Fernandez-Gamiz, A. Saenz-Aguirre, and R. Martinez, "Predictive dynamic window approach development with artificial neural fuzzy inference improvement," *Electronics*, vol. 8, no. 9, p. 935, 2019.

[60] M. Bhardwaj, B. Boots, and M. Mukadam, "Differentiable gaussian process motion planning," *arXiv preprint arXiv:1907.09591*, 2019.

[61] X. Xiao, Z. Wang, Z. Xu, B. Liu, G. Warnell, G. Dhamankar, A. Nair, and P. Stone, "Appl: Adaptive planner parameter learning," *Robotics and Autonomous Systems*, vol. 154, p. 104132, 2022.

[62] X. Xiao, B. Liu, G. Warnell, J. Fink, and P. Stone, "Appld: Adaptive planner parameter learning from demonstration," *IEEE Robotics and Automation Letters*, vol. 5, no. 3, pp. 4541–4547, 2020.

[63] Z. Wang, X. Xiao, B. Liu, G. Warnell, and P. Stone, "Appli: Adaptive planner parameter learning from interventions," in *2021 IEEE international conference on robotics and automation (ICRA)*. IEEE, 2021, pp. 6079–6085.

[64] Z. Wang, X. Xiao, G. Warnell, and P. Stone, "Apple: Adaptive planner parameter learning from evaluative feedback," *IEEE Robotics and Automation Letters*, vol. 6, no. 4, pp. 7744–7749, 2021.

[65] Z. Xu, G. Dhamankar, A. Nair, X. Xiao, G. Warnell, B. Liu, Z. Wang, and P. Stone, "Applr: Adaptive planner parameter learning from reinforcement," in *2021 IEEE international conference on robotics and automation (ICRA)*. IEEE, 2021, pp. 6086–6092.

[66] Z. Xu, X. Xiao, G. Warnell, A. Nair, and P. Stone, "Machine learning methods for local motion planning: A study of end-to-end vs. parameter learning," in *2021 IEEE International Symposium on Safety, Security, and Rescue Robotics (SSRR)*. IEEE, 2021, pp. 217–222.

[67] "move_base – ros wiki," http://wiki.ros.org/move_base, accessed: 2023-06-24.

[68] "social_navigation_layers - ros wiki," http://wiki.ros.org/social_navigation_layers, accessed: 2023-06-25.

[69] P. T. Singamaneni and R. Alami, "Hateb-2: Reactive planning and decision making in human-robot co-navigation," in *International Conference on Robot & Human Interactive Communication*, 2020.

[70] L. T. Triess, M. Dreissig, C. B. Rist, and J. M. Zöllner, "A survey on deep domain adaptation for lidar perception," *2021 IEEE Intelligent Vehicles Symposium Workshops (IV Workshops)*, pp. 350–357, 2021. [Online]. Available: https://api.semanticscholar.org/CorpusID:235352671

[71] D. A. Pomerleau, "Alvinn: An autonomous land vehicle in a neural network," in *Advances in neural information processing systems*, 1989, pp. 305–313.